CHEMISTRY
A EUROPEAN JOURNAL

DOI: 10.1002/chem.200501078

Fluorine Segregation in Crystalline Materials: Structural Control and Solid-State [2+2] Cycloaddition in CF_3-Substituted Tetrathiafulvalene Derivatives

Olivier Jeannin and Marc Fourmigué*[a]

Abstract: The well-known influence of long perfluorinated chains on the structures and stability of amphiphilic molecules in liquid crystalline mesophases or mesoscopic micellar arrangements is evaluated here in the realm of crystalline materials based on rigid aromatic molecules bearing only a limited number of CF_3 moieties. Tetrathiafulvalene (TTF) derivatives bearing one or two CF_3 groups, that is, (*Z*)- and (*E*)-$(CF_3)_2$TTF ((*Z*)-**1**, (*E*)-**1**), EDT-TTF-CF_3 (**2**), and EDT-TTF$(CF_3)_2$ (**3**) (EDT = ethylenedithio) are prepared from the 1,3-dipolar reaction of methyl 4,4,4-trifluorotetrolate with ethylenetrithiocarbonate. The structures of neutral (*Z*)-**1**, (*E*)-**1**, **2,** and **3** as indicated by single-crystal X-ray diffraction measurements reveal the recurrent formation of layered structures with a strong segregation of the fluorinated moieties and formation of fluorous bilayers, attributed to the amphiphilic character of those TTF derivatives upon CF_3 functionalization, and without need for longer C_nF_{2n+1} ($n>1$) perfluorinated chains. The short intermolecular distance between outer C=C double bonds observed in the layered structure of (*E*)-**1** allows a solid-state [2+2] photocyclization with formation of chiral dyads incorporating the characteristic cyclobutane ring. These dyads containing two dihydrotetrathiafulvalene moieties facing each other exhibit reversible oxidation to the mixed-valence radical cation state and organize in the solid-state into the same layered structures with fluorous bilayers.

Keywords: crystal engineering · cycloaddition · fluorine · layered compounds · tetrathiafulvalene

Introduction

The control of solid-state architectures of molecular organic solids through directional, strong intermolecular interactions such as hydrogen[1] or halogen[2] bonds forms the basis of supramolecular solid-state chemistry,[3] a very successful approach that has allowed a very fine control of supramolecular solid-state architectures. In that respect, little attention has been given to the exclusive use of nondirectional van der Waals interactions for the targeted construction of ordered architectures of specific dimensionality, that is, the selective crystallization into chains, columns, layers, or three-dimensional ordered structures of organic molecules devoid of any functional group for hydrogen (alcohols, acids, amides, amines, and so forth), or halogen (Cl, Br, I) bonding, π–π aryl/perfluoroaryl interactions, or metal coordination. On the other hand, this approach is routinely used in soft-matter chemistry, where amphiphilic molecules with a strong incompatibility between the different parts adopt a variety of mesophase morphologies based on the segregation of hydrophilic versus hydrophobic but also rigid versus flexible fragments.[4] When available, crystals of such amphiphilic molecules often exhibit layered structures based on these segregation effects.[5] Replacement of alkyl chains with fluorinated or semifluorinated chains has become very popular since mesophases are stabilized due to the increased incompatibility of such chains with the aromatic cores.[6,7] Furthermore, a variety of novel mesophase topologies are introduced, as observed in ABC triblock copolymers,[8] linear polyphilic block molecules,[9,10] or calamitic molecules with both terminal and lateral chains.[11] The combined hydro- and lipophobia of fluorinated compounds can be used to generate complex nano- to mesomeric phases[12] such as segregated micelles,[13] liposomes,[14] and bidimensional films.[15] Also, the successful incorporation of trifluoro-[16] or hexafluoroleucine[17] as the sole hydrophobic core residue in a designed coiled coil provided the very first examples of highly specific protein–protein interaction based on fluorination of the hydrophobic core.

We wanted to take advantage of such segregation effects of fluoroaliphatic groups in crystalline molecular materials

[a] O. Jeannin, Dr. M. Fourmigué
Laboratoire Chimie, Ingénierie Moléculaire et Matériaux (CIMMA)
UMR 6200 CNRS-Université d'Angers
Bât K, UFR Sciences
2 Bd Lavoisier, 49045 Angers, (France)
Fax: (+33) 241-735-405
E-mail: marc.fourmigue@univ-angers.fr

to obtain controlled solid-state organizations. For example, long perfluorinated chains directly linked to oligo-[18] and polythiophenes[19] have a strong influence on molecular packing and the absorption and emission spectra,[20] enable solubility[21] in supercritical CO_2, and afford n-dopable semiconductors.[22] Among conducting materials, semifluorinated tetrathiafulvalene (TTF) derivatives have been prepared for Langmuir–Blodgett film formation,[23] while incorporation of highly fluorinated anions such as $(CF_3)_3CF(CH_2)_2$-SO_3^- in TTF salts also stabilized the formation of layered materials.[24,25] The very strong contrast offered by fluoroaliphatics in polymer science, biochemistry, and soft-matter chemistry let us infer that even single CF_3 groups rather than long C_nF_{2n+1} perfluoroalkyl chains, adequately positioned on the rigid core, could be sufficient to provide a segregation and formation of layered crystalline structures, as very recently observed in hexafluoroacetylacetonate (hfac) complexes.[26] Indeed, the two-dimensional structures often encountered in cation radical salts are also highly desirable in the structures of the neutral TTF-like donor molecules if one is interested in the design of crystalline thin films for transistor devices.[27] A more systematic investigation should produce a selection of the best molecules for producing high-quality thin films with high intralayer mobilities.[22] We therefore decided to prepare various aromatic cores substituted with a limited number of the shortest perfluorinated chain, that is, the trifluoromethyl group, and selected the tetrathiafulvalene (TTF) backbone as a useful candidate for CF_3 functionalization. Indeed, among the few TTF-based donor molecules with aliphatic fluorine moieties, the only crystallographically characterized examples already indicate an efficient segregation of the fluorinated moieties, as observed in: 1) tetrakis-(trifluoromethyl)-tetrathiafulvalene $(CF_3)_4$TTF,[28] 2) TTF molecules substituted with 2,2′-difluoropropylene-1,3-dithio groups such as $(F_2PDT)_2$TTF,[29] and very recently, 3) nickel dithiolene complexes of bis(trifluoromethyl)tetrathiafulvalenedithiolate moieties.[30]

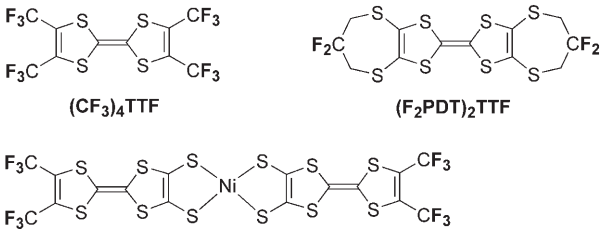

For example, the crystal structure of $(CF_3)_4$TTF as derived from X-ray crystallography (Figure 1), exhibits a pseudo-columnar arrangement with the outer surface of each stack being essentially covered with fluorine atoms. The columns organize in the solid in a close-packed hexagonal structure, very similar to those observed in liquid-crystalline discotic CoI_h phases. These examples demonstrate that the introduction of CF_3 or CF_2 moieties on the rigid TTF core can induce a molecular contrast strong enough to force a micro-

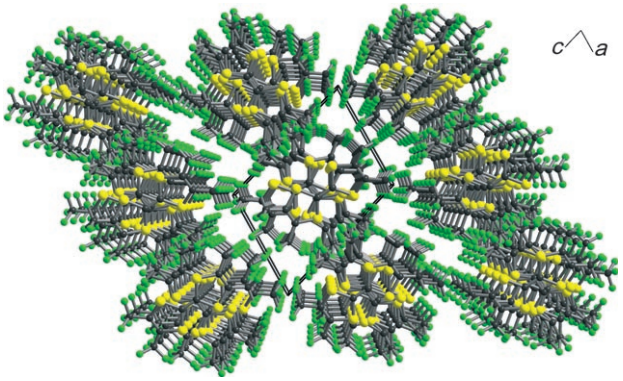

Figure 1. The structural organization of $(CF_3)_4$TTF, viewed along the *b* stacking axis (fluorine atoms are shown in green).

segregation of the fluorinated and aromatic moieties. To evaluate the robustness of this segregation principle, we decided to investigate the functionalization of the rigid TTF core with only one or two CF_3 moieties, to evaluate the influence on the solid-state structure of the neutral donor molecules of the successive introduction of CF_3 moieties on different positions of the TTF core.

We describe the synthesis of TTF derivatives **1–3** that have been substituted by mono- and bis(trifluoromethyl)

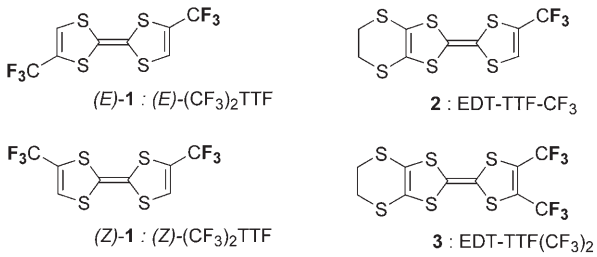

moieties, the determination and analysis of their X-ray crystal structures, and their electrochemical properties. We also show that this specific fluorine segregation can favor a close proximity between TTF derivatives in the crystal, that are thus prone to a solid-state [2+2] cycloaddition reaction under irradiation, leading to a rare example of a dimeric donor molecule with a rigid cyclobutane bridge and strongly interacting, redox-active, dihydrotetrathiafulvanyl moieties.

Results and Discussion

Synthesis: $TTF(CF_3)_4$ is the only tetrathiafulvalene derivative described so far that includes a trifluoromethyl substituent linked directly to the TTF core. The preparations described are based on the reaction of the volatile hexafluorobutyne either with CS_2,[31] metal complexes thereof as [(triphos)Ni(η^2-CS_2)] (triphos = 1,1,1-tris(diphenylphosphinomethyl)ethane),[32] or with boiling sulfur to give the corresponding bis(trifluoromethyl)dithiete[33] for further reaction.

The preparations are therefore limited to this specific derivative, together with the added inconvenience of the availability and handling of this gaseous alkyne. On the other hand, the 1,3-dipolar-addition reaction of activated acetylenes with ethylenetrithiocarbonate has proven to be one of the main routes in tetrathiafulvalene chemistry[34] since it affords, often in very good yield, 1,3-dithiole-2-thiones for further phosphate-or phosphine-coupling reactions to the TTF derivatives. For the introduction of only one CF_3 group on the dithiole ring, we therefore chose to start from the trifluoromethyl-substituted alkyne **6**, where the presence of two electron-withdrawing groups, an ester and a trifluoromethyl group, should confer a good reactivity towards ethylenetrithiocarbonate, as was observed (see below).

The methyl ester of the alkyne **6** was prepared according to a procedure described for its ethyl analog,[35] from triphenylphosphine oxide (Ph_3PO) elimination of the corresponding phosphoranylidene **5**, as shown in Scheme 1, and isolated after distillation as a clear liquid. Reaction with ethylenetrithiocarbonate under reflux in toluene afforded the corresponding dithiole-2-thione **7** in good yield (Scheme 2). The latter was the starting material for the preparation of trifluoromethyl-substituted TTF derivatives since the carbomethoxy group(s) can be easily removed by reaction with LiBr in DMF,[36] as shown in Scheme 2 for the synthesis of the

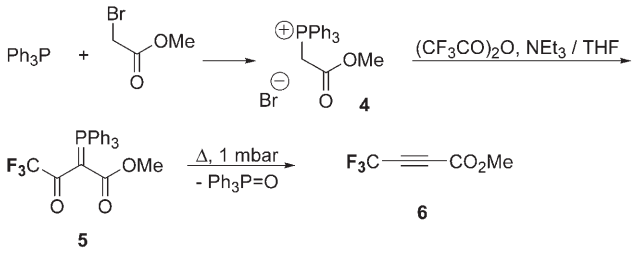

Scheme 1.

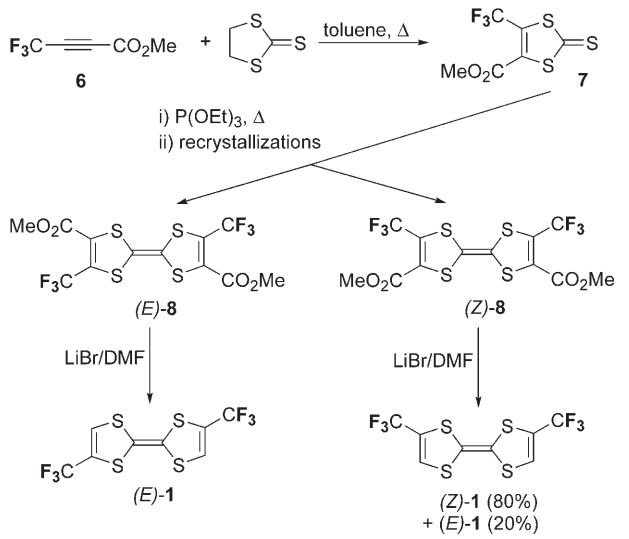

Scheme 2.

bis(trifluoromethyl)tetrathiafulvalenes (*E*)-**1** and (*Z*)-**1**. Indeed, the phosphite-coupling reaction of the 1,3-dithiole-2-thione **7** afforded the bis-trifluoromethyl-bis-carbomethoxytetrathiafulvalene **8** as a *Z*-*E* isomeric mixture. The two isomers were separated by successive recrystallizations from methanol, affording first the less-soluble (*E*)-**8** isomer, while the more-soluble (*Z*)-**8** isomer was obtained from the mother liquors. Both compounds appear to be pure as shown by TLC. Treatment of isolated isomers with LiBr in warm DMF led to decarboxylation and both *E*-**1** and (*Z*)-**1** were obtained in 63 (*E*) and 88 (*Z*)% yield, respectively. We observed that (*Z*)-**1** was obtained but also that partial isomerization to (*E*)-**1** occurred during the decarboxylation of (*Z*)-**8**, since the final product contains 15–20% of *E* isomer, as deduced from NMR spectrum as well as the X-ray crystal structure of (*Z*)-**1** (see below). The high solubility and close polarity of both isomers did not allow for a complete purification of the *Z* isomer.

Similarly, as shown in Scheme 3, following the transformation of the 1,3-dithiole-2-thione **7** into the corresponding dithiole-2-one **9** with $Hg(OAc)_2$, the cross-coupling reaction of

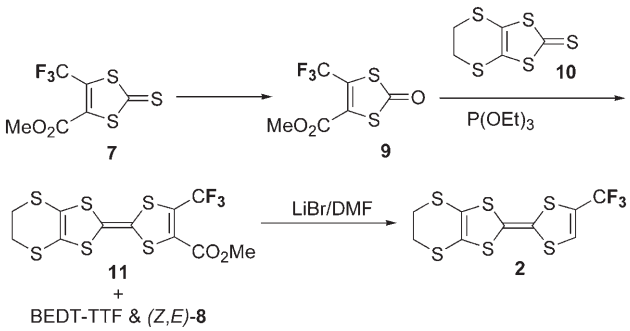

Scheme 3.

9 with 5,6-dihydro-[1,3]dithiolo[4,5-*b*][1,4]dithiine-2-thione **10** afforded the asymmetrically substituted EDT–TTF derivative **11** bearing both the carbomethoxy and trifluoromethyl substituents, separated from the symmetrical-coupling products BEDT-TTF and (*Z*,*E*)-**8** by chromatography. Treatment of **11** with LiBr in warm DMF[36] afforded the trifluoromethyl EDT–TTF derivative **2** in good yield, isolated in a crystalline form after recrystallization.

The synthesis of the bis(trifluoromethyl) EDT-TTF derivative EDT-TTF$(CF_3)_2$ (**3**) relies on a similar phosphite coupling of 5,6-dihydro-[1,3]dithiolo[4,5-*b*][1,4]dithiine-2-one[37] **10** with 4,5-bis(trifluoromethyl)1,3-dithiole-2-thione **12** as described in Scheme 4. The latter has been prepared following a described procedure involving the nucleophilic displacement of chlorine atoms in 2,3-dichloro-1,1,1,4,4,4-hexafluoro-2-butene with K_2CS_3.[38] (*Z*)-**1**, (*E*)-**1**, **2**, and **3** are highly soluble in all common solvents excluding water. They were satisfactorily recrystallized from EtOH/H_2O mixtures.

Solid-state structures: **toward fluorine segregation**: Let us first consider the trifluoromethyl EDT-TTF derivative **2**

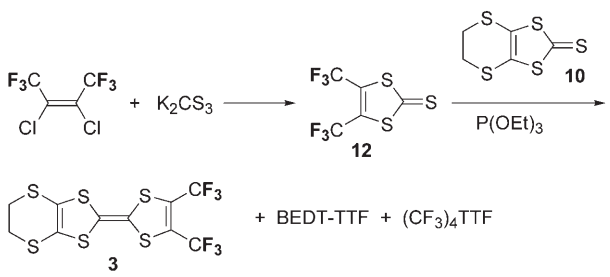

Scheme 4.

bearing only one CF_3 group. It crystallizes in the monoclinic system, space group $P2_1/c$, with one molecule in a general position in the unit cell. Of particular note is the strong folding of the two dithiole rings, 23.28(15)° on the dithioethylene side, 20.99(14)° on the CF_3 side. In the solid state (Figure 2), molecules associate into inversion-centered

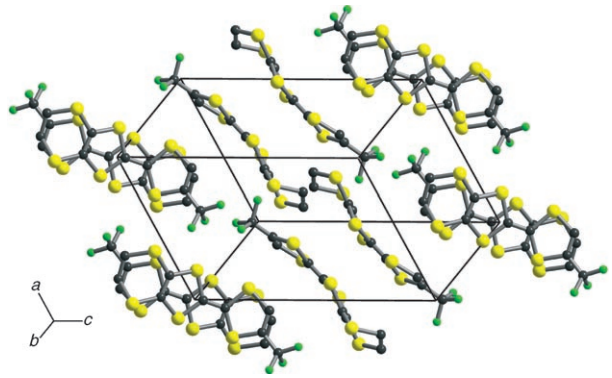

Figure 2. Solid-state arrangement of compound **2**, showing the dyadic association (fluorine atoms are shown in green).

dyads, a recurrent feature among neutral, nonsubstituted EDT-TTF derivatives such as EDT-TTF itself,[39] BEDT-TTF,[40] and others,[41] demonstrating that the S···S van der Waals interactions that stabilize these dyads essentially overcome possible fluorine segregation effects here, as also confirmed by the absence of any F···F short distances below 3 Å. On the other hand, a segregation of the fluorinated moieties is readily observed in the TTF derivatives bearing two CF_3 groups, as indeed observed in EDT-TTF$(CF_3)_2$ (**3**), (*Z*)- and (*E*)-$(CF_3)_2$TTF, ((*Z*)-**1** and (*E*)-**1**). EDT-TTF$(CF_3)_2$ (**3**) crystallizes in the monoclinic system, space group $P2_1/n$, with two crystallographically independent molecules A and B in the asymmetric unit that differ from each other by a disorder of the ethylenic moiety and a strong folding of the dithiole ring bearing the two CF_3 moieties (30°) in one of the two molecules. In the solid state, molecules A and B associate into AB head-to-tail dyads (Figure 3). Alternating ABABAB stacks form along axis *b*, and organize laterally along the *a* axis through S···S van de Waals contacts to form slabs with a striking segregation of the fluorinated moieties at the interface between slabs (Figure 4), giving rise to the

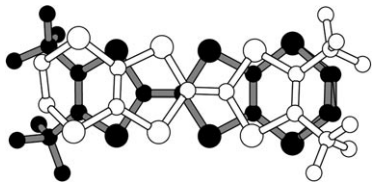

Figure 3. Detail of the bond-over-ring overlap between A and B molecules in the stacks of compound **3**.

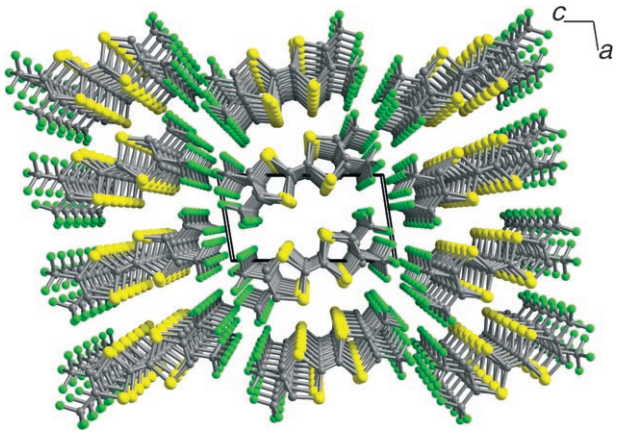

Figure 4. Solid-state organization of EDT-TTF$(CF_3)_2$ (**3**) showing the fluorine segregation (fluorine atoms are shown in green).

formation of fluorous bilayers. Such layered structures are most often found in the mixed-valence conducting BEDT-TTF salts with alternating organic and inorganic layers but are almost never found in structures of neutral donor molecules unless cohesive interactions stabilize the interface between layers, as observed for example in the structure of neutral dithienotetrathiafulvalene[42] with S···S van der Waals interactions or in the neutral EDT-TTF$(CONH_2)_2$ diamide with a set of hydrogen-bond interactions.[43] Here in derivative **3**, the planarity of the central TTF core, the stacking of the molecules, and the association of stacks within a layered structure occur only on the basis of the incompatibility between different parts of the molecules, without any stabilizing intermolecular interactions such as hydrogen bonds.

In other words, the functionalization of the highly polarizable (soft) sulfur-containing EDT-TTF core in derivative **3** with two weakly polarizable (hard) CF_3 substituents provides the molecule with a strong amphiphilic character. As a consequence, the energy of its solid-state associations is expected to be lowest if both opposite fragments segregate, in order to suppress direct contacts between fragments of opposite polarity as far as possible. It is also noteworthy that this specific bilayer formation is observed here with a very limited number of CF_3 moieties while the few described examples involved longer perfluoroaliphatic C_nF_{2n+1} ($n=5$) chains.[44]

The (*Z*)- and (*E*)-$(CF_3)_2$TTF (*Z*)-**1** and (*E*)-**1** derivatives also display an amphiphilic character but with a completely

different topology when compared with derivative **3** since the two CF_3 moieties are now on opposite sides of the rigid TTF core. The noncentrosymmetric (*Z*)-**1** isomer crystallizes in the monoclinic system, space group *I*2/*a*. Note that the CF_3 groups are found disordered on the four outer C atoms of the TTF core, which could correspond to a 90:10 distribution of the two possible orientations, or better to an 80:20 mixture of the *Z* and *E* isomers, as already identified from the NMR data. In the solid state, molecules related by inversion centers (Figure 5) alternate into stacks running along

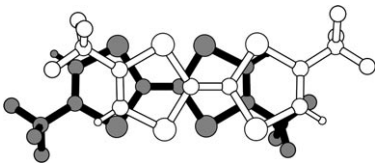

Figure 5. Detail of the bond-over-ring overlap between derivative (*Z*)-**1** molecules in the stacks.

axis *b*. Combination of the stacks along axis *c* affords a layered structure organization, again with fluorinated bilayers (Figure 6), similar to those observed in the structure of de-

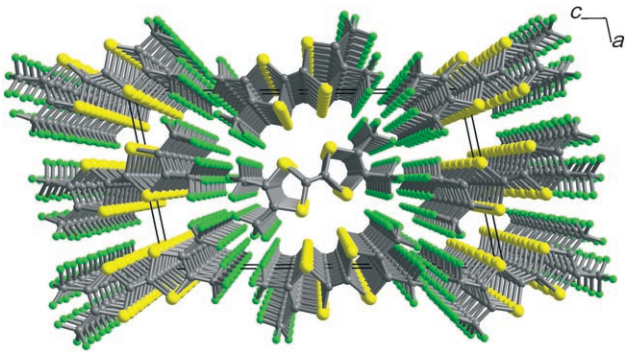

Figure 6. Solid-state organization of (*Z*)-$(CF_3)_2$TTF ((*Z*)-**1**) showing the fluorine segregation (fluorine atoms are shown in green).

rivative **3**. In (*E*)-$(CF_3)_2$TTF, two crystallographically independent molecules A and B, each located on an inversion center crystallize in the triclinic system, space group $P\bar{1}$. They form alternating ABABAB stacks along the *b* axis (Figure 7), further interacting through S···S van der Waals forces into slabs, separated from each other by the fluorine double layer (Figure 8).

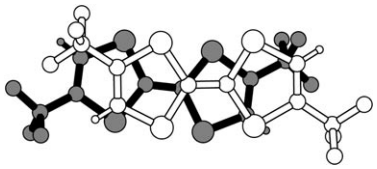

Figure 7. Detail of the overlap between A and B molecules in (*E*)-$(CF_3)_2$TTF ((*E*)-**1**).

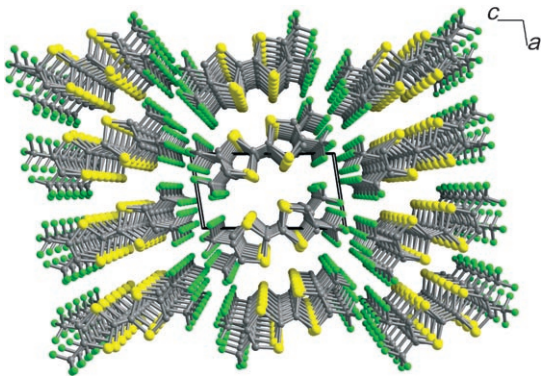

Figure 8. Solid-state organization of (*E*)-$(CF_3)_2$TTF ((*E*)-**1**) showing the fluorine segregation (fluorine atoms are shown in green).

The analogy between the structures of derivatives **3**, (*Z*)-**1**, and (*E*)-**1** despite different locations of the CF_3 moieties on the rigid core, is due to the recurrent tendency of the TTF core to form bond-over-ring dyads through S···S van der Waals interactions (Figures 3, 5, and 7). As a consequence, a similar bimolecular motif incorporating two rigid cores and four CF_3 groups (Scheme 5), located on both ends of the dyad, is found at the origin of the comparable solid-state organizations in the three structures shown in Figures 4, 6, and 8.

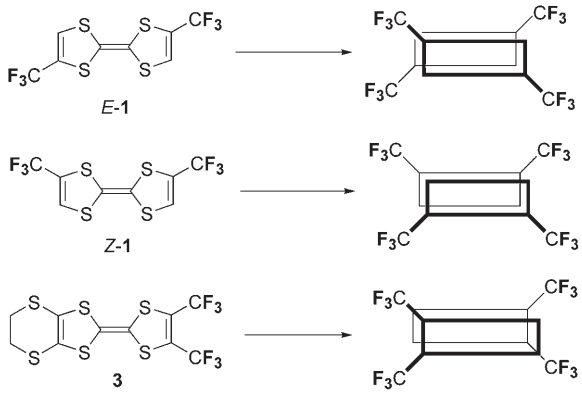

Scheme 5. Solid-state organization of derivatives (*E*)-**1**, (*Z*)-**1**, and **3** into a recurrent inversion-centered dyadic motif bearing four CF_3 moieties.

The lamellar topologies observed in the structures of derivatives (*Z*)-**1**, (*E*)-**1**, and **3** infer that they could eventually exhibit mesophases upon heating. While derivatives (*Z*)- and (*E*)-**1** do not exhibit any special feature, the differential scanning calorimetry (DSC) thermogram of derivative **3** shows, before the fusion peak at 168 °C (55.5 $J\,g^{-1}$), a pre-peak at 120 °C, but with a low enthalpy (3.8 $J\,g^{-1}$) attributable to a crystal–crystal transition. Direct observation through a polarizing microscope showed no evidence of any birefringent fluid phase upon slowly heating solid compound **3** or slowly cooling **3** from its melt.[45]

Solid-state [2+2] cycloaddition: We also observed that crystals of derivative (*E*)-**1** kept in sunlight slowly changed color from orange to yellow within a few days and simultaneously slowly lost their crystallinity, while those kept in the dark remained unchanged for months. MALDI-TOF experiments on this yellow powder showed the presence, besides the starting TTF derivative (*E*)-**1**, of a compound of double mass (679.74 uma) and some degradation products. Since the crystallinity of (*E*)-**1** was lost upon irradiation, the recovered solid was recrystallized in EtOH to afford a compound denoted (*EE*)-**13** in the form of elongated thin plates, together with minor quantities of other compounds. A second experiment with Hg-lamp irradiation, followed by successive column chromatography with CH_2Cl_2 and CS_2, and recrystallization of the mixture from CH_3CN, afforded two other compounds denoted (*EZ*)-**13** and (*ZZ*)-**13**. A combination of ^1H and ^{19}F NMR, and X-ray crystal-structure determinations on the three products allowed the unambiguous determination of their molecular structures, demonstrating that a [2+2] photocyclization of derivative (*E*)-**1** had taken place to afford compound (*EE*)-**13**. The product exhibits ^1H NMR signals at 5.80 ppm (in [D_6]acetone) attributable to a cyclobutane ring while signals due to two different CF_3 groups were observed in ^{19}F NMR spectra, also compatible with a [2+2] photocyclization involving the outer C=C double bond of the TTF core. Compound (*EE*)-**13** crystallizes in the orthorhombic system, space group $P222_1$ with one molecule located on a twofold axis (Figure 9). The chiral

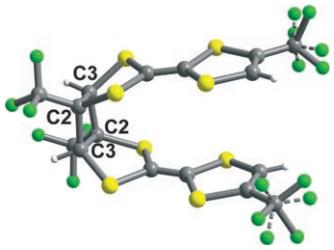

Figure 9. A view of derivative (*EE*)-**13**. Cyclobutane moiety characteristics: C2–C3: 1.571(7), C2–C3^i: 1.584(7) Å; C2-C3-C2^i: 90.0(4), C3-C2-C3^i: 89.5(4)° (i: −x, y, 0.5−z). The two orientations of the disordered CF_3 groups have been marked with normal and dashed bonds.

nature of the $P222_1$ space group let us infer that one single isomer is present but refinement of the Flack parameter converged to 0.47(19) during refinement cycles. The somewhat large esd on the Flack parameter might originate from the weakness of the anomalous dispersion effect since the sulfur atoms (the only substantial anomalous scatterers) form pseudocentrosymmetric motifs in the structure. On the other hand, this Flack parameter value can also indicate the presence of racemic twinning.[46] Indeed, a rationale for the formation of two enantiomers during the [2+2] photocyclization can be found in the peculiar organization of derivative (*E*)-**1** in the solid state (Figure 10). Two crystallographically independent molecules, denoted A and B, each of them located on an inversion center, stack along the *b* axis.

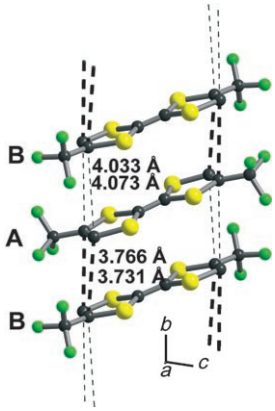

Figure 10. Detail of the solid-state organization of derivative (*E*)-**1**.

While the C_6S_4-TTF core in molecule B is essentially planar (largest deviation from the C_6S_4 mean plane: 0.03 Å), molecule A is more distorted with the dithiole rings folded along the S···S hinge by 8.36(8)°. As a consequence, the intermolecular distances between the carbon atoms of the outer C=C double bonds cluster into two groups, 3.731(4) and 3.766(4) Å on one side, 4.033(4) and 4.073(4) on the other side. The [2+2] photocyclization takes place between nearest C=C double bonds, affording either one or the other isomer, as shown in Scheme 6. These two possibilities of-

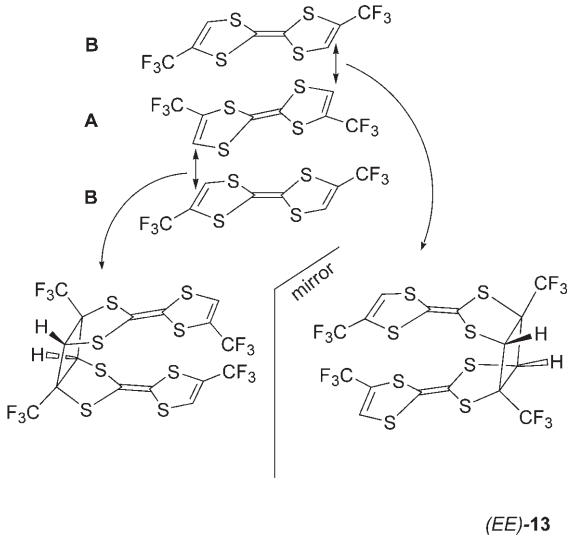

Scheme 6. [2+2] Photodimerization of derivative (*E*)-**1** upon single-crystal irradiation.

fered for a given molecule for the [2+2] photodimerization most probably explain the loss of crystallinity of the compound during irradiation, since many defaults can be anticipated. Note also that this process could eventually lead to oligomeric species linked by cyclobutane motifs. Indeed, once a pair of molecules reacts, each end of the dimer still has a double bond that could undergo a second [2+2] cyclization to give a longer oligomer. Such species were not ob-

served by MS analysis on irradiated crystals of derivative (*E*)-**1**.

This [2+2] photocyclization is similar to that observed upon irradiation of carbamoyl tetrathiafulvalenes[47,48] as well as an amidopyridyl tetrathiafulvalene formulated as EDT-TTF-CONH(3-Py)[49] where a single-crystal-to-single-crystal transformation was revealed due to a favorable orientation of the molecules through π–π interactions. Following the pioneering work of Schmidt on the [2+2] photodimerization of cinnamic acids,[50] several geometrical rules have been established as guidelines for evaluating the possible occurrence of such dimerizations.[51] Considering the *D* distance, θ_1, θ_2, and θ_3 angles defined in Table 1, it is normally expected that photocyclizations might occur if $D <$ 4.2 Å, θ_1 is close to 0°, θ_2 and θ_3 are close to 90°, the most stringent condition being that the two C=C double bonds are essentially parallel, that is θ_1 is close to 0°. Values of *D*, θ_1, θ_2, and θ_3 are presented in Table 1 for derivative (*E*)-**1**, together with those for derivatives (*E*)-**1**, **3**, and the only other described example, EDT-TTF-CONH(3-Py). They confirm the favorable geometry for dimerization in derivative (*E*)-**1** or EDT-TTF-CONH(3-Py) and we can infer that similar cyclizations could also be observed in derivatives (*Z*)-**1** or **3**.

Table 1. Geometrical characteristics of the TTF dyads before [2+2] cyclization.

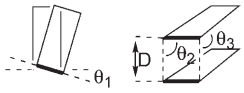

Compound	*D* [Å]	θ_1 [°]	θ_2 [°]	θ_3 [°]	Ref.
(*E*)-**1**	3.75	9.2	94.3	72.8	this work
	4.05	9.3	98.6	74.3	
(*Z*)-**1**	3.79	3.5	91.0	71.0	this work
3	3.81	3.3	90.3	75.8	this work
EDT-TTF-CONH(3-Py)	3.54	0	71.6	77.8	[48]

Indeed, irradiation of derivative (*Z*)-**1** also led to a partial discoloration of the crystals. However, chromatographic separation allowed the isolation of (*EE*)-**13** in only 1.6% yield, while the starting (*Z*)-**1** compound was recovered essentially unaltered. Similarly, irradiation of derivative **3** was also attempted given the close proximity (3.82 Å) between the outer C=C double bonds of the dithiole ring bearing the S-CH_2CH_2-S moiety and the dithiole ring bearing the two CF_3 groups. No color change was observed and the crystals remained unchanged, demonstrating the lack of reactivity of the ethylene-rich $(RS)_2C{=}C(SR)_2$ system.

Two other compounds were obtained after attempted chromatographic separations and recrystallizations of compound (*EE*)-**13**. They both exhibit the cyclobutane proton signals, at $\delta = 5.786$ and 5.795 ppm for compound (*EZ*)-**13** (two signals) and $\delta = 5.82$ ppm (in [D_6]acetone) for compound (*ZZ*)-**13**, while signals due to two CF_3 groups are observed with ^{19}F NMR spectroscopy in compound (*ZZ*)-**13** and four CF_3 groups in compound (*EZ*)-**13**. The latter compound was found to crystallize in the monoclinic system, space group *P*2/*n*, with one molecule in a general position in the unit cell (Figure 11). It indeed displays the cyclobutane

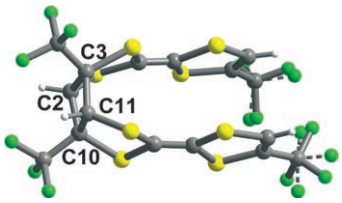

Figure 11. A view of derivative (*ZE*)-**13**. Cyclobutane moiety bond lengths [Å] and angles [°]: C2–C3 1.559(4), C10–C11 1.568(4), C2–C10 1.568(4), C3–C11 1.579(4); C2-C3-C11 89.4(2), C10-C11-C3 89.5(2), C3-C2-C10 90.2(2), C2-C10-C11 89.2(2). The two orientations of the disordered CF_3 groups have been marked with normal and dashed bonds.

ring characteristic of the [2+2] cycloaddition but in one of the two dihydrotetrathiafulvalene moieties, the two CF_3 groups are now found in a *cis* configuration to each other, implying that an isomerization has taken place. Such isomerizations of the central C=C double bond of the TTF core are often observed,[52] catalyzed by traces of acid or on SiO_2 columns. Indeed, protonation of the central double bond allows for a free rotation of the dithiole rings, affording compound (*ZE*)-**13** from (*EE*)-**13** (Scheme 7). This process

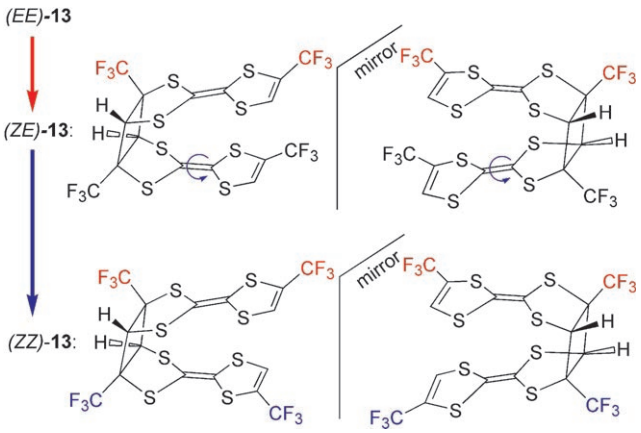

Scheme 7. Isomerization of derivatives (*EE*)-**13** to (*ZE*)-**13** and (*ZZ*)-**13** through rotation around the central C=C bonds.

was already observed here (vide infra) during the preparation of derivative (*Z*)-**1** to afford a fraction of derivative (*E*)-**1**. By the way, the crystallization of compound (*ZE*)-**13** in a centrosymmetric space group confirms the presence of both enantiomers in the starting (*EE*)-**13** compound, as anticipated from the presence of racemic twinning in compound (*EE*)-**13**. The third compound (*ZZ*)-**13** corresponds to the structure where both CF_3 groups of each dihydrotetrathiafulvalene moiety are now found in a *cis* configuration to each other, implying that a second isomerization from compound (*ZE*)-**13** to (*ZZ*)-**13** has also taken place.

Besides providing a rare example of [2+2] photocyclization in TTF chemistry, the solid-state structures of compounds (*EE*)-**13** and (*ZE*)-**13** also offer another opportunity to evaluate the robustness of the segregation principle developed above. As a matter of fact, the bimolecular motifs bearing four CF_3 moieties identified in the structures of derivatives **3**, (*E*)-**1**, and (*Z*)-**1** (Scheme 5) occur in compounds (*EE*)-**13** and (*ZE*)-**13**. Indeed, despite different unit cell parameters and symmetry characteristics, their solid-state arrangement (Figures 12 and 13) still exhibit the recurrent layered structures with strong fluorine segregation, further exemplifying the ability of this dyadic motif to stabilize the formation of layered crystals with these characteristic fluorine bilayers.

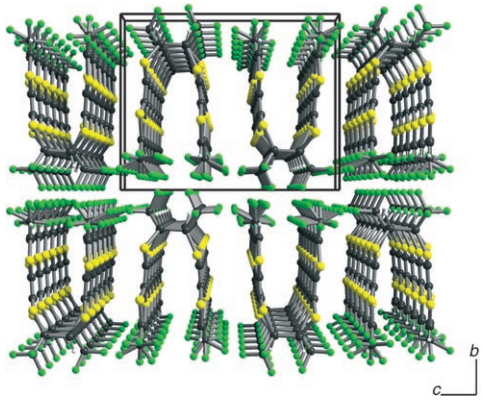

Figure 12. Solid-state organization of derivative (*EE*)-**13** showing the fluorine segregation (fluorine atoms are shown in green).

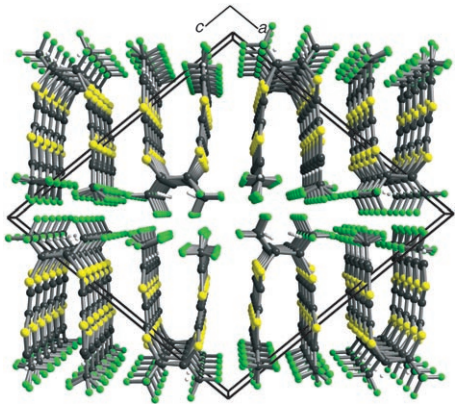

Figure 13. Solid-state organization of derivative (*ZE*)-**13** showing the fluorine segregation (fluorine atoms are shown in green).

In conclusion, the specific organization of derivative (*E*)-**1** within the columns and the softness of the lattice provided by the weakly interacting fluorous layers allowed a remarkable solid-state transformation, but also provided a novel molecular motif where two dihydrotetrathiafulvalene moieties are now constrained to face each other, a case model for all TTF dimers[53] and cyclophanes[54] described to date where multi-stage redox behavior was expected from the face-to-face interaction between the two redox-active moieties.

Electrochemical properties of the trifluoromethyl-substituted TTF derivatives and their [2+2] cycloaddition adduct: Since the tetrakis(trifluoromethyl)tetrathiafulvalene, $(CF_3)_4$TTF, oxidizes at high potential due to the presence of the four electron-withdrawing CF_3 groups, we were interested to evaluate the influence of only one or two such CF_3 groups on the redox properties of the TTF core, also to determine the air-stability of the corresponding cation radical salts. The TTF derivatives **1**–**3** described here exhibit the two characteristic reversible oxidation waves (Table 2), to

Table 2. Redox potentials for compounds **1**–**3** and reference compounds, in V versus Fc^+/Fc. Values for reference compounds reported against SCE have been corrected by −0.40 V for comparison purposes.

Compound	Solvent	E_1[V]	E_2[V]	Ref.
EDT-TTF	CH_3CN	0.04	0.35	[39]
EDT-TTF-CF_3 (**2**)	CH_2Cl_2	0.21	0.64	this work
EDT-TTF$(CF_3)_2$ (**3**)	CH_2Cl_2	0.37	0.76	this work
TTF	CH_3CN	-0.07	0.31	[55]
(*E*)-**1**	CH_2Cl_2	0.40	0.78	this work
(*Z*)-**1**	CH_2Cl_2	0.40	0.78	this work
TTF$(CF_3)_4$	CH_2Cl_2	0.65	0.88	[31]

the mono and dicationic species. Note that the introduction of one electron-withdrawing CF_3 group on each dithiole ring, as in derivatives (*E*)-**1** and (*Z*)-**1**, leads to a strong anodic shift (+ 0.47 V) of the first oxidation potential of the TTF core[55] while the introduction of two CF_3 groups on the same dithiole ring as in derivative **3** induces a smaller (+0.33 V) shift. To evaluate the extent of intramolecular interactions between the two dihydrotetrathiafulvalene moieties in the cyclobutane-linked dimers **13**, the major (*EE*)-**13** product was also investigated by cyclic voltammetry (Figure 14). Two reversible oxidation waves (Table 3) are observed at 0.69 and 0.88 V versus Fc^+/Fc, followed by an

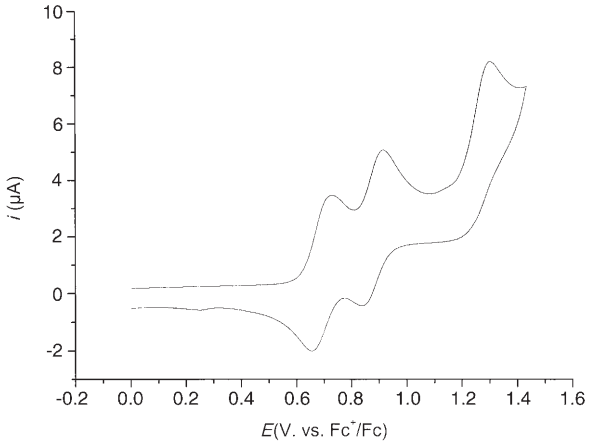

Figure 14. Cyclic voltammetry results of derivative (*EE*)-**13** (1.4 mM in CH_2Cl_2 with nBu_4NPF_6 0.2 M).

Table 3. Redox potentials for compound (*EE*)-**13** and reference compounds.

Compound	Solvent	Reference	E_1[V]	E_2[V]	E_2-E_1[mV]	E_3[V]	Ref.
TTF	CH_3CN	SCE	0.33	–	–	0.71	[55]
$TTFH_2$	CH_3CN	SCE	0.405	–	–	0.89	[54]
(*E*)-**1**	CH_2Cl_2	Fc^+/Fc	0.40	–	–	0.78	this work
(*EE*)-**13**	CH_2Cl_2	Fc^+/Fc	0.69	0.88	190	1.26	this work
14	PhCN	INIST	0.28	0.41	130	0.90	[56]
15	PhCN	Ag/Ag^+	0.57	0.67	100	1.15	[57]
16	PhCN	Ag/AgCl	0.57	0.70	130	0.98	[58]
17	PhCN	Ag/AgCl	0.41	0.56	150	0.83	[59]

irreversible process at 1.26 V, indicating that each dihydrotetrathiafulvalene moiety in compound (*EE*)-**13** oxidizes successively to the cation radical. The first oxidation potential of the dihydro derivative (*EE*)-**13** appears at a more anodic potential (+290 mV) than that of the corresponding fully conjugated TTF derivative (*E*)-**1**. This anodic shift due to the loss of conjugation upon cyclobutane formation is much larger than that observed between TTF and dihydrotetrathiafulvalene ($TTFH_2$) themselves (+75 mV). Furthermore, the separation (ΔE) of 190 mV between the two first oxidation processes in compound (*EE*)-**13** indicates a strong intramolecular interaction between the two dihydrotetrathiafulvalenyl redox centers.

This ΔE value largely exceeds those reported for comparable TTF dimers and cyclophanes such as compounds **14**–**17** (Scheme 8 and Table 3) where the two TTF redox centers

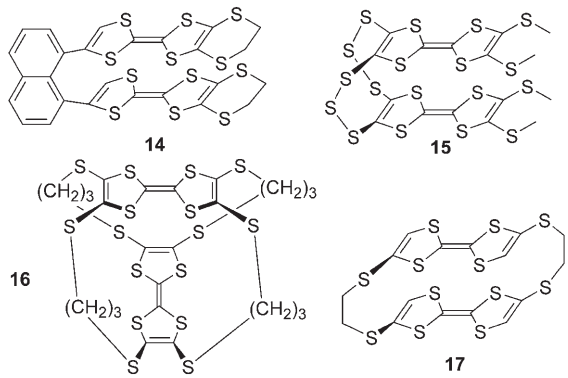

Scheme 8. Examples of TTF dimers and cyclophanes exhibiting face-to-face interactions and sequential one-electron redox processes (see Table 3).

are constrained in a face-to-face conformation.[56–59] The main difference between compounds **14**–**17** and compound (*EE*)-**13** is in the very close proximity of the redox moieties in compound (*EE*)-**13** due to the cyclobutane ring and also in its increased rigidity while molecules **14**–**17** still exhibit degrees of freedom.

Conclusion

We have demonstrated here, by using the rigid TTF core, that a very limited number of trifluoromethyl groups was sufficient to induce a strong amphiphilic character in aromatic molecules, while other examples of such segregation effects with similar fluorous bilayer formation rely on molecules bearing long C_nF_{2n+1} ($n=5$) perfluoroalkyl chains. This concept appears to be extremely robust since molecules with diverse CF_3 locations as in derivatives (*Z*)-**1**, (*E*)-**1**, and **3** systematically produce such layered structures, built from a recurrent bimolecular motif, almost identical to that also formed upon [2+2] photocyclization. It is therefore expected that many aromatics functionalized with a limited number of CF_3 moieties might exhibit similar layered structures, an important feature in the search for n-dopable molecular semiconductors, an issue of current strong interest.[18,22]

Furthermore, the photodimerization of derivative (*E*)-**1** represents a very first example of a solid-state transformation involving molecules whose relative positioning is controlled only by the segregation of fluoroaliphatic moieties. Indeed, in most examples described so far of crystalline solid-state reactions such as the polymerization of diacetylenes or the [2+2] cycloaddition of alkenes, the favorable orientation of molecules is achieved either by serendipity or purposely through the involvement of directional intermolecular interactions such as hydrogen bonding,[60] halogen bonding,[61] or π–π interactions.[48,62] Here, the relative orientation of the two TTF moieties is obtained within a layered structure occurring due to the amphiphilic character of the molecules.

The resulting photocyclization product includes two redox-active dihydrotetrathiafulvalene moieties, constrained in a face-to-face structure through the short and rigid cyclobutane fragment, an original feature that allows an unprecedented, strong intramolecular interaction evidenced by their large potential difference between the two first oxidation potentials.

Experimental Section

All reagents were commercially available unless otherwise stated. Nuclear magnetic resonance spectra were recorded at 500.04 MHz for ^1H and 125.75 MHz for ^{13}C NMR spectroscopy (s: singlet; q: quadruplet). Mass spectrometry was performed in the MALDI-TOF mode except for compounds **7** and **9** that were analyzed in the High Resolution (HR) mode. (Carbomethoxymethyl)triphenylphosphonium bromide **4** was prepared as described in reference [63], bis(trifluoromethyl)-1,3-dithiole-2-thione **12** was prepared as described in reference [38], and 5,6-dihydro-[1,3]dithiolo[4,5-*b*][1,4]dithiine-2-one **10** as described in reference [37].

Methyl 4,4,4-trifluoro-2-(triphenylphosphoranylidene)acetoacetate (5): NEt_3 (130 mL, 0.93 mol) was slowly added to a suspension of compound **4** (184 g, 0.44 mol) in dry THF at 0 °C under nitrogen atmosphere. The mixture was stirred for 1 h at 0 °C. Trifluoroacetic anhydride (100 g, 0.47 mol) was added dropwise at 0 °C over about 1.5 h. Stirring was maintained for 2 h before the suspension was filtered. The white precipitate

was washed with cold THF (500 mL) and the mother liquors were concentrated. The oily residue was triturated in water (1 L), filtered, and was washed with water (1 L) to give a pale-yellow solid. After recrystallization in a methanol/water mixture, the product was obtained as very pale yellow crystals (183.93 g, 96%).

^{1}H NMR ($CDCl_3$): $\delta = 3.3$ (s, 3H), 7.48 (m, 6H), 7.58 (m, 3H), 7.66 ppm (m, 6H); ^{31}P NMR ($CDCl_3$): $\delta = 19.9$ ppm (s); elemental analysis calcd (%) for $C_{23}H_{18}F_3O_3$: C 63.95, H 4.21; found: C 64.19, H 4.22.

Methyl 4,4,4-trifluorotetrolate (6): Compound **5** (193 g, 0.45 mol) was pyrolyzed by slowly warming under reduced-pressure (1 mbar) up to 160–165 °C when it started to melt. The distillate was condensed in a Dewar condenser cooled with liquid N_2 gas. The pale yellow liquid was dried over magnesium sulfate and was distilled at 39 °C under 208 mbar pressure to give the acetylenic derivative as a colorless liquid (106.19 g; 80.5%). Owing to the instability of the compound, it was not stored but was directly used in the cycloaddition reaction with ethylenetrithiocarbonate to afford compound **6**.

^{1}H NMR ($CDCl_3$): $\delta = 3.87$ (s, 3H); ^{13}C NMR ($CDCl_3$): $\delta = 54.3$ (s, CH_3), 71.04 (q, $^2J_{C,F} = 54.7$ Hz; *C*-CF_3), 75.97 (q, $^3J_{C,F} = 6.41$ Hz; *C*CO_2Me), 114.12 (q, $^1J_{C,F} = 260.3$ Hz; CF_3), 151.83 ppm (s, C=O); ^{19}F NMR ($CDCl_3$): $\delta = -52.80$ ppm (s, CF_3).

4-Carbomethoxy-5-trifluoromethyl-1,3-dithiol-2-thione (7): Freshly prepared methyl 4,4,4-trifluorotetrolate **6** (66.16 g, 0.43 mol) and ethylenetrithiocarbonate (59.27 g, 0.43 mol) were warmed under reflux for 24 h under N_2 atmosphere in dry toluene (310 mL). The solvent was then evaporated and the residue was purified by chromatography on SiO_2, and eluted with pentane/dichloromethane (4:1) to afford the yellow dithiolethione **7**, after recrystallization from methanol (145.4 g, 74.4%); m.p. 33 °C (MeOH); ^{1}H NMR ($CDCl_3$): $\delta = 3.92$ ppm (s, 3H); ^{13}C NMR ($CDCl_3$): $\delta = 53.96$ (s, Me), 118.07 (q, $^1J_{C,F} = 275.52$ H; *C*F_3), 137 (s, *C*–(CO_2Me)), 136.98 (q, $^2J_{C,F} = 39.23$ Hz; *C*–CF_3), 156.17 (s, C=O), 204.79 ppm (s, C=S); ^{19}F NMR ($CDCl_3$): $\delta = -55.66$ ppm (s, CF_3); elemental analysis calcd (%) for $C_6H_3F_3O_2S_3$: C 27.43, H 1.07; found: C 27.68, H 1.16; HRMS: *m*/*z*: calcd: 259.9247; found: 259.9241.

(*Z*-*E*)-Bis-trifluoromethyl-bis-carbomethoxytetrathiafulvalene ((*E*)-8 and (*Z*)-8): Compound **7** (0.81 g, 3.15 mmol) was dissolved in dry toluene (15 mL) and treated with 2.25 equivalents of trimethylphosphite (0.84 mL, 7.1 mmol). The mixture was refluxed under N_2 gas for 2 h. The solvent was then evaporated and the solid residue triturated in hot methanol (25 mL). After cooling and filtration, a red-purple powder (0.24 g) was obtained. This sample showed two spots with TLC (petroleum ether/dichloromethane 2:1) attributed to the two isomers. The filtrate was purified by chromatography on SiO_2 and was eluted with petroleum ether/dichloromethane (2:1) to give 0.23 g of the two isomers. The global yield of the *Z*-*E* mixture was 0.57 g (65%). Elemental analysis calcd (%) for $C_{12}H_6F_6O_4S_4$: C 31.58, H 1.32; found: C 31.76, H 1.31; MS: *m*/*z*: calcd: 455.905; found: 455.97. The two isomers were separated after several recrystallizations in methanol to give the pure (TLC) *Z* and *E* isomers. (*Z*)-**8**: m.p. 102–104 °C; ^{1}H NMR ($CDCl_3$): $\delta = 3.89$ ppm (s, 6H); ^{13}C NMR ($CDCl_3$): $\delta = 53.53$ (s), 108.49 (s), 119.19 (q, $^1J_{C,F} = 273$ Hz), 130.89 (s), 132.51 (q, $^2J = 38$ Hz), 157.61 ppm (s); ^{19}F NMR ($CDCl_3$): $\delta = -56.11$ ppm (s). (*E*)-**8**: m.p. 188–195 °C; ^{1}H NMR ($CDCl_3$): $\delta = 3.89$ ppm (s, 6H); ^{13}C NMR ($CDCl_3$): $\delta = 53.59$ (s), 108.54 (s), 119.203 ppm (q, $^1J_{C,F} = 275$ Hz), 130.7 (s), 132.63 (q, $^2J = 38.60$ Hz), 157.59 ppm (s); ^{19}F NMR ($CDCl_3$): $\delta = -56.11$ ppm (s).

(*Z*- and *E*)-Bis(trifluoromethyl)tetrathiafulvalene ((*E*)-1 and (*Z*)-1): Typical procedure: pure (TLC) (*Z*)-**8** or (*E*)-**8** isomers (0.3 g, 0.66 mmol) and LiBr (1 g) were dissolved in DMF (10 mL). The mixture was heated at 80 °C for 6 h. After cooling, water (100 mL) was added to precipitate the product. After filtration and drying, the crude product was recrystallized in an ethyl alcohol/water mixture to give orange needles. The filtrate was purified by chromatography on SiO_2 and eluted with pentane/dichloromethane (8:1). The global yield was 0.14 g (63%) for the (*E*)-**1** isomer and 0.19 g (88%) for isomer (*Z*)-**1**. (*Z*)-**1**: ^{1}H NMR ($CDCl_3$): $\delta = 6.89$ ppm (s); ^{13}C NMR ($CDCl_3$): $\delta = 111.27$ (s, *C*=*C*), 119.82 (q, $^1J_{C,F} = 269.9$ Hz; CF_3,), 124.23 (q, $^2J_{C,F} = 38.4$ Hz; *C*CF_3), 124.78 ppm (q, $^3J_{C,F} = 5.8$ Hz; *C*H); ^{19}F NMR ($CDCl_3$): $\delta = -60.92$ ppm (s); elemental analysis calcd (%) for $C_8H_2F_6S_4$: C 28.23, H 0.59; found: C 28.72, H 0.64; MS: calcd: 339.89; found: 339.17. (*E*)-**1**: ^{1}H NMR ($CDCl_3$): $\delta = 6.89$ ppm (s); ^{13}C NMR ($CDCl_3$): $\delta = 111.18$ (s, *C*=*C*), 119.82 (q, $^1J_{C,F} = 269.9$ Hz; CF_3,), 124.36 (q, $^2J_{C,F} = 37.5$ Hz; *C*CF_3), 124.59 ppm (q, $^3J_{C,F} = 5.1$ Hz; *C*H); ^{19}F NMR ($CDCl_3$): $\delta = -60.92$ ppm (s); elemental analysis calcd (%) for $C_8H_2F_6S_4$: C 28.23, H 0.59; found: C 28.30, H 0.62; MS: calcd: 339.89; found: 339.17.

4-Carbomethoxy-5-trifluoromethyl-1,3-dithiol-2-one (9): Compound **7** (5.22 g, 0.02 mol) was dissolved in a chloroform/acetic acid mixture (3:1, 800 mL). Mercuric acetate (12.89 g, 0.04 mol) was added and the mixture was stirred under nitrogen atmosphere for 2.5 h. The white precipitate was filtered through Celite and was washed with dichloromethane. The filtrate was washed with a saturated $NaHCO_3$ solution and then with water. The yellow precipitate that appeared during the washing was not added to the organic phase. After drying over magnesium sulfate, solvents were evaporated to give compound **9** as a salmon-colored oil (4.53 g, 91%). ^{1}H NMR ($CDCl_3$): $\delta = 3.92$ ppm (s, 3H); ^{13}C NMR ($CDCl_3$): $\delta = 53.86$ (s, CH_3), 118.91 (q, $^1J_{C,F} = 273.5$ Hz; *C*F_3), 128.83 (q, $^3J_{C,F} = 3$ Hz; *C*-(CO_2Me)), 130.03 (q, $^2J_{C,F} = 38.4$ Hz; *C*-CF_3), 157.31 (s, *C*(=O)OMe), 184.41 ppm (s, *C*=O); ^{19}F NMR ($CDCl_3$): $\delta = -54.88$ ppm (s); elemental analysis calcd (%) for $C_6H_3F_3O_3S_2$: C 29.51, H 1.24; found: C 29.74, H 1.33.

4,5-Ethylenedithio-4′-carbomethoxy-5′-trifluoromethyltetrathiafulvalene (11): Compounds **9** (0.5 g, 1.14 mmol) and **10** (0.46 g, 2.05 mmol) were slowly heated up to 110 °C in trimethylphosphite (24 mL) under a nitrogen atmosphere. After 160 min at 110 °C, the mixture was concentrated to half the original volume and was cooled to 4 °C before filtration of the precipitated BEDT-TTF. The filtrate was evaporated and purified by chromatography on SiO_2 and was eluted with petroleum ether/ethyl acetate (3:1) to give first the mixture of *Z*-*E* diesters **8** (0.16 g, 17%) followed by the desired compound **11**, obtained as a dark-purple powder (0.45 g, 52%). The product was recrystallized in ethanol to give compound **11** as purple platelets (0.33 g, 38%); m.p. 108 °C (EtOH); ^{1}H NMR ($CDCl_3$): $\delta = 3.31$ (s, 4H), 3.85 ppm (s, 3H); ^{13}C NMR ($CDCl_3$): $\delta = 30.197$ (s, *C*H_2*C*H_2), 53.46 (s, Me), 112.19 (s), 113.94 (s), 114.17 (s), 119.36 (q, $^1J_{C,F} = 274.51$ Hz; CF_3), 130.52 (s, *C*-CO_2Me), 132.58 (q, $^2J_{C,F} = 76.46$ Hz; *C*-CF_3), 157.89 ppm (s, *C*OOMe); ^{19}F NMR ($CDCl_3$): $\delta = -56.3$ ppm (s); elemental analysis calcd for $C_{11}H_7F_3O_2S_6$: C 31.41, H 1.68; found: C 31.57, H 1.65; MS: *m*/*z*: calcd: 419.87; found: 419.93.

4,5-Ethylenedithio-4′-trifluoromethyltetrathiafulvalene (2): Compound **11** (0.48 g, 1.14 mmol) and LiBr (1.2 g) were heated at 80 °C for 7 h in DMF (25 mL) under nitrogen. The mixture was then poured into distilled water (100 mL) and the orange precipitate was filtered off. After drying, the product was recrystallized in isopropanol to give compound **2** (0.31 g, 75.6%) as orange flakes; m.p. 109.6 °C (*i*PrOH); ^{1}H NMR ($CDCl_3$): $\delta = 3.3$ (s, 4H), 6.86 ppm (q, $^4J_{H,F} = 1.41$ Hz, 1H); ^{13}C NMR ($CDCl_3$): $\delta = 30.12$ (s, *C*H_2*C*H_2), 109.848 (s), 113.43 (s), 113.89 (s), 114.08 (s), 119.9 (q, $^1J_{C,F} = 271.37$ Hz; CF_3), 123.99 (q, $^2J_{C,F} = 37.47$ Hz; *C*-CF_3), 124.621 ppm (t, $^1J_{C,H} = 5.28$ Hz; =*C*-H); ^{19}F NMR ($CDCl_3$): $\delta = -60.3$ ppm (s); elemental analysis calcd (%) for $C_6H_5F_3S_6$: C 29.82, H 1.39; found: C 29.66, H 1.29; HRMS: *m*/*z*: calcd: 361.86; found: 361.1.

Bis(trifluoromethyl)ethylendithiotetrathiafulvalene (3): 4,5-Bis(trifluoromethyl)-1,3-dithiole-2-thione **12** (0.43 g, 1.67 mmol) and compound **10** (0.41 g, 1.83 mmol) were heated in trimethylphosphite (15 mL) under a nitrogen atmosphere. After 2 h at 110 °C, the mixture was evaporated and toluene (15 mL) was added. The suspension was triturated and filtered to give BEDT-TTF (0.1 g, 14.5%). The filtrate was evaporated and purified by chromatography on silica gel and was eluted with petroleum ether/dichloromethane (3:1) to give first the orange tetrakis(trifluoromethyl)tetrathiafulvalene (0.17 g, 22%) followed by the desired product **3** (0.11 g, 16%); m.p. 168.7 °C (hexane); ^{1}H NMR ($CDCl_3$): $\delta = 3.31$ ppm (s, 4H); ^{13}C NMR ($CDCl_3$): $\delta = 30.20$ (s, *C*H_2-*C*H_2), 105.62 (s), 114.71 (s), 114.63 (s), 118.9 (q, $^1J_{C,F} = 275.64$ Hz; CF_3), 128.443 ppm (q, $^2J_{C,F} = 42$ Hz; *C*-CF_3); ^{19}F NMR ($CDCl_3$): $\delta = -56.82$ ppm (s); elemental analysis calcd (%) for $C_{10}H_4F_6S_6$: C 27.90, H 0.94; found: C 27.83, H 0.76; HRMS: *m*/*z*: calcd: 429.85; found: 429.84.

Cyclization product (13): Orange crystals of compound (*E*)-**1** that were allowed to stand in the sunlight for two weeks at room temperature slowly lost their crystallinity and turned yellow. The starting TTF deriva-

tive (*E*)-**1** was eliminated by washing with pentane. Recrystallization in EtOH afforded derivative (*EE*)-**13** as elongated thin plates together with a microcrystalline yellow powder. ^{19}F and ^{1}H NMR measurements on this mixture revealed the presence of about 20% of product (*ZZ*)-**13**.

In a second experiment, single crystals of derivative (*E*)-**1** were irradiated for two days in a sealed tube with a 400-W Hg-lamp with regular manual shaking of the sample. The product was purified by silica-gel chromatography (first column with CH_2Cl_2 elution, second column with CS_2 elution) but afforded a mixture of compounds (*EE*)-**13** and (*ZZ*)-**13** in a 30:70 ratio according to ^{19}F NMR. Recrystallization of this mixture in CH_3CN yielded yellow plates of compound (*ZE*)-**13** according to the X-ray diffraction experiment. Concentration of the mother liquors afforded a few crystals, identified by X-ray diffraction as compound (*ZZ*)-**13**. Mother liquors still contained 52% of compound (*ZE*)-**13**, 40% of compound (*EE*)-**13**, and 8% of compound (*ZZ*)-**13c.**

NMR data in $CDCl_3$: Derivative (*EE*)-**13**: ^{1}H NMR ($CDCl_3$): $\delta = 5.14$ (s, C−*C*−*H*), 6.7 ppm (s, C=*C*−*H*); ^{19}F NMR ($CDCl_3$): $\delta = -60.64$ (s, C=C−*CF*$_3$), −73.26 ppm (s, C−C−*CF*$_3$). Derivative (*ZE*)-**13**: ^{19}F NMR ($CDCl_3$): $\delta = -59.88$ (s, C=C−*CF*$_3$), −61.40 (s, C=C−*CF*$_3$), −73.48 (s, C−C−*CF*$_3$), −73.55 ppm (s, C−C−*CF*$_3$). Derivative (*ZZ*)-**13**: ^{1}H NMR ($CDCl_3$): $\delta =$ 5.14 (s, C−*C*−*H*), 6.81 ppm (s, C=*C*−*H*); ^{19}F NMR ($CDCl_3$): $\delta = -61.25$ (s, C=C−*CF*$_3$); −73.22 ppm (s, C−C−*CF*$_3$).

NMR data in [D_6]acetone: Derivative (*EE*)-**13**: ^{1}H NMR ([D_6]acetone): $\delta = 5.8$ (s, C−*C*−*H*); 7.48 ppm (q, $^{4}J_{F,H} = 1.36$ Hz; C=*C*−*H*); ^{19}F NMR ([D_6]acetone): $\delta = -61.27$ (s, C=C−*CF*$_3$), −74.02 ppm (s, C−C−*CF*$_3$). Derivative (*ZE*)-**13**: ^{1}H NMR ([D_6]acetone): $\delta = 5.786$ (s, 1H; C−*C*−*H*), 5.795 (s, 1H; C−*C*−*H*), 7.39 (q, 1H; C=*C*−*H*), 7.47 ppm (q, 1H; C=*C*−*H*); ^{19}F NMR ([D_6]acetone): $\delta = -60.56$ (s, 3F; C=C−*CF*$_3$), −62.03 (s, 3F; C=C−*CF*$_3$), −74.05 (s, 3F; C−C−*CF*$_3$), −74.08 ppm (s, 3F; C−C−*CF*$_3$). Derivative (*ZZ*)-**13**: ^{1}H NMR ([D_6]acetone): $\delta = 5.82$ (s, C−*C*−*H*), 7.47 ppm (q, C=*C*−*H*); ^{19}F NMR ([D_6]acetone): $\delta = -61.7$ (s; C=C−*CF*$_3$), −73.86 ppm (s, C−C−*CF*$_3$); MS: *m*/*z*: calcd: 679.79; found: 679.74.

Crystal structure determinations: Crystals were mounted on top of a thin glass fiber. Data were collected on a Stoe Image-Plate Diffraction System (IPDS) or an Enraf Nonius Kappa CCD with graphite-monochromated $Mo_{K\alpha}$ radiation ($\lambda = 0.71073$ Å). The crystal data are summarized in Table 4. Structures were solved by direct methods (SHELXS-97) and refined (SHELXL-97) by full-matrix least-squares methods. Absorption corrections were applied for all structures. Hydrogen atoms were introduced at calculated positions (riding model), were included in structure factor calculations, and not refined. CCDC 282792–282797 contain the supplementary crystallographic data for this paper. These data can be obtained free of charge from The Cambridge Crystallographic Data Centre via www.ccdc.cam.ac.uk/data_request/cif.

Electrochemistry: Cyclic voltammetry was performed in dry CH_2Cl_2 with 0.1 M (nBu$_4$N)(PF_6) at a scan rate of 100 mV s^{-1}, with an Ag/$AgNO_3$ reference electrode. The ferricinium/ferrocene system was used as internal reference.

[1] G. A. Jeffrey, W. Saenger, W. *Hydrogen Bonding in Biological Structures*, Springer, Berlin, **1991**.
[2] a) J. P. M. Lommerse, A. J. Stone, R. Taylor, F. H. Allen, *J. Am. Chem. Soc.* **1996**, *118*, 3108; b) P. Metrangolo, G. Resnati, *Chem. Eur. J.* **2001**, *7*, 2511; c) R. S. Walsh, C. W. Padgett, P. Metrangolo, G. Resnati, T. W. Hanks, W. T. Pennington, *Cryst. Growth Des.* **2001**, *1*, 165.
[3] a) G. R. Desiraju, *Angew. Chem.* **1995**, *107*, 2505; *Angew. Chem. Int. Ed. Engl.* **1995**, *34*, 2311; b) G. R. Desiraju, *Crystal Engineering: The Design of Organic Solids*, Elsevier, Amsterdam, **1989**; c) J. L. Atwood, J. M. Lehn, J. E. D. Davies, D. D. MacNicol, F. Vogtle, *Comprehensive Supramolecular Chemistry*, Pergamon Press, **1996**.
[4] For a recent review, see: C. Tschierske, *J. Mater. Chem.* **2001**, *11*, 2647.
[5] W. Haase, N. A. Athanassopoulou, *Struct. Bonding (Berlin)* **1999**, *94*, 139.
[6] a) P. Kromm, H. Allouchi, J. P. Bideau, M. Cotrait, *Mol. Cryst. Liq. Cryst.* **1994**, *257*, 9; b) P. Kromm, H. Allouchi, J. P. Bideau, M. Cotrait, H. T. Nguyen, *Acta Crystallogr. Sect. C* **1995**, *51*, 1229.
[7] X. H. Cheng, S. Diele, C. Tschierske, *Angew. Chem.* **2000**, *112*, 605; *Angew. Chem. Int. Ed.* **2000**, *39*, 592.
[8] I. W. Hamley, *The Physics of Block Copolymers*, Oxford University Press, Oxford, **1998**.

Table 4. Crystallographic data.

Compound	**2**	**3**	(*E*)-**1**	(*Z*)-**1**	(*EE*)-**13**	(*ZE*)-**13**
formula	$C_9H_5F_3S_6$	$C_{10}H_4F_6S_6$	$C_8H_2F_6S_4$	$C_8H_2F_6S_4$	$C_{16}H_4F_{12}S_8$	$C_{16}H_4F_{12}S_8$
f_w	362.49	430.53	340.34	340.34	680.67	680.67
cryst syst	monoclinic	monoclinic	triclinic	monoclinic	orthorhombic	monoclinic
space group	$P2_1/c$	$P2_1/n$	$P\bar{1}$	$I2/a$	$P222_1$	$P2/n$
a [Å]	9.8622(11)	12.7780(10)	6.3953(10)	12.730(3)	6.7094(5)	18.4374(10)
b [Å]	8.4530(7)	8.1930(19)	7.7454(13)	7.7000(15)	11.6717(9)	6.6670(2)
c [Å]	16.0641(19)	27.946(5)	11.956(2)	23.588(5)	14.7671(10)	18.8335(16)
α [°]	90	90	97.81(2)	90	90	90
β [°]	102.82(1)	93.330(10)	97.399(19)	101.60(3)	90	101.221(7)
γ [°]	90	90	100.456(19)	90	90	90
V [Å^{-3}]	1305.8(2)	2920.7(9)	569.82(16)	2264.9(8)	1156.41(15)	2270.8(2)
Z	4	8	2	8	2	4
ρ_{calcd} [Mg m^{-3}]	1.844	1.958	1.984	1.996	1.955	1.991
diffractometer	Stoe-IPDS	Kappa CCD	Stoe-IPDS	Stoe-IPDS	Kappa CCD	Kappa CCD
T[K]	150(2)	150(2)	150(2)	150(2)	293(2)	293(2)
μ [mm^{-1}]	1.058	0.991	0.888	0.894	0.875	0.891
θ-range [°]	2.12–25.86	2.59–27.50	1.74–25.86	1.76–25.65	2.22–27.50	2.20–27.0
measd reflns	9837	46038	5383	10213	8945	74490
independent reflns	2520	6590	2003	2047	2529	4954
R_{int}	0.0406	0.0614	0.0425	0.0359	0.0772	0.0624
$I > 2\sigma(I)$ refls	2177	4815	1713	1716	1976	3569
abs corr	multi-scan	multi-scan	multi-scan	multi-scan	multi-scan	multi-scan
T_{max},T_{min}	0.839, 0.661	1.0, 0.727	1.14, 0.773	0.746, 0.643	1.174, 0.778	1.0, 0.8994
refined parameters	167	416	171	225	190	379
$R(F)$, $I > 2\sigma(I)$	0.030	0.0452	0.0335	0.0339	0.0476	0.0392
$wR(F^2)$, all	0.0761	0.1104	0.0918	0.1049	0.1639	0.1248
$\Delta\rho$ [e Å^{-3}]	+0.48, −0.27	+0.74, −0.43	+0.33, −0.35	+0.37, −0.37	+0.72, −0.89	+0.51, −0.4

[9] a) F. Guittard, E. Taffin de Givenchy, S. Geribaldi, A. Cambon, *J. Fluorine Chem.* **1999**, *100*, 85; b) M.-A. Guillevic, D. W. Bruce, *Liq. Cryst.* **2000**, *27*, 153.
[10] S. Pensec, F.-G. Tournilhac, P. Bassoul, C. Durliat, *J. Phys. Chem. B* **1998**, *102*, 52.
[11] S. V. Arehart, C. Pugh, *J. Am. Chem. Soc.* **1997**, *119*, 3027.
[12] M.-P. Krafft, *Curr. Opin. Colloid Interface Sci.* **2003**, *8*, 213.
[13] a) P. Mukerjee, A. Y. S. Yang, *J. Phys. Chem.* **1976**, *80*, 1388; b) K. Stähler, J. Selb, F. Candau, *Langmuir* **1999**, *15*, 7565; c) A. Laschewsky, *Curr. Opin. Colloid Interface Sci.* **2003**, *8*, 274.
[14] R. Elbert, T. Folda, H. Ringsdorf, *J. Am. Chem. Soc.* **1984**, *106*, 7687.
[15] M.-P. Krafft, M. Goldmann, *Curr. Opin. Colloid Interface Sci.* **2003**, *8*, 243.
[16] B. Bilgiçer, A. Fichera, K. Kumar, *J. Am. Chem. Soc.* **2001**, *123*, 4393.
[17] B. Bilgiçer, X. Xing, K. Kumar, *J. Am. Chem. Soc.* **2001**, *123*, 11815.
[18] a) A. Facchetti, Y. Deng, A. Wang, Y. Koide, H. Sirringhaus, T. J. Marks, R. H. Friend, *Angew. Chem.* **2000**, *112*, 4721; *Angew. Chem. Int. Ed.* **2000**, *39*, 4547; b) A. Facchetti, M. Mushrush, H. E. Katz, T. J. Marks, *Adv. Mater.* **2003**, *15*, 33; c) A. Facchetti, J. Letizia, M.-H. Yoon, M. Mushrush, H. E. Katz, T. J. Marks, *Chem. Mater.* **2004**, *16*, 4715.
[19] A. Facchetti, M. Mushrush, M.-H. Yoon, G. R. Hutchison, M. A. Ratner, T. J. Marks, *J. Am. Chem. Soc.* **2004**, *126*, 13859.
[20] L. Li, D. M. Collard, *Macromolecules* **2005**, *38*, 372.
[21] L. Li, K. E. Counts, S. Kurowasa, A. S. Teja, D. M. Collard, *Adv. Mater.* **2004**, *16*, 180.
[22] S. Ando, J. Nishida, H. Tada, Y. Inoue, S. Tokito, Y. Yamashita, *J. Am. Chem. Soc.* **2005**, *127*, 5336.
[23] C. Mingotaud, B. Agricole, T. Nozdryn, J. Cousseau, A. Gorgues, P. Delhaes, *Thin Solid Films* **1997**, *300*, 228.
[24] U. Geiser, J. A. Schlüter, A. Kini, H. H. Wang, B. H. Ward, J. Mohtasham, G. L. Gard, *Synth. Met.* **2003**, *133–134*, 401.
[25] U. Geiser, J. A. Schlüter, *Chem. Rev.* **2004**, *104*, 5203.
[26] S. R. Halper, S. M. Cohen, *Inorg. Chem.* **2005**, *44*, 4139.
[27] a) M. Mas-Torrent, M. Durkut, P. Hadley, X. Ribas, C. Rovira, *J. Am. Chem. Soc.* **2004**, *126*, 984; b) S. T. Bromley, M. Mas-Torrent, P. Hadley, C. Rovira, *J. Am. Chem. Soc.* **2004**, *126*, 6544.
[28] S. Mono, H. Pritzkow, W. Sundermeyer, *Chem. Ber.* **1993**, *126*, 2111.
[29] O. J. Dautel, M. Fourmigué, *J. Org. Chem.* **2000**, *65*, 6479.
[30] M. Sasa, E. Fujiwara, A. Kobayashi, S. Ishibashi, K. Terakura, Y. Okano, H. Fujiwara, H. Kobayashi, *J. Mater. Chem.* **2005**, *15*, 155.
[31] H. D. Hartzler, *J. Am. Chem. Soc.* **1973**, *95*, 4379.
[32] C. Bianchini, A. Meli, *J. Chem. Soc. Chem. Commun.* **1983**, 1309.
[33] C. G. Krespan, B. C. McKusick, T. L. Cairns, *J. Am. Chem. Soc.* **1960**, *82*, 1515.
[34] A. Gorgues, M. Sallé, P. Hudhomme, *Chem. Rev.* **2004**, *104*, 5151.
[35] B. C. Hamper, *Org. Synth.* **1992**, *70*, 246.
[36] R. P. Parg, J. D. Killburn, M. C. Petty, C. Pearson, T. G. Ryan, *J. Mater. Chem.* **1995**, *5*, 1609.
[37] J. Larsen, C. Lenoir, *Synthesis* **1989**, 134.
[38] C. G. Krespan, D. C. England, *J. Org. Chem.* **1967**, *32*, 1850.
[39] B. Gareau, D. de Montauzon, P. Cassoux, J.-P. Legros, J.-M. Fabre, K. Saoud, S. Chakroune, *New J. Chem.* **1995**, *19*, 161.
[40] H. Kobayashi, A. Kobayashi, Y. Sasaki, G. Saito, H. Inokuchi, *Bull. Chem. Soc. Jpn.* **1986**, *59*, 301.
[41] C. Mézière, M. Fourmigué, J.-M. Fabre, *C. R. Acad. Sci. Paris, Série IIC, Chimie* **2000**, *3*, 387.
[42] C. Rovira, J. Veciana, N. Santaló, J. Tarrés, J. Cirujeda, E. Molins, J. Llorca, E. Espinosa, *J. Org. Chem.* **1994**, *59*, 3307.
[43] S. A. Baudron, N. Avarvari, P. Batail, C. Coulon, R. Clérac, E. Canadell, P. Auban-Senzier, *J. Am. Chem. Soc.* **2003**, *125*, 11583.
[44] See, for example: a) F. C. Krebs, H. Spangaard, *J. Org. Chem.* **2002**, *67*, 7185; b) C. Rocaboy, F. Hampel, J. A. Gladysz, *J. Org. Chem.* **2002**, *67*, 6863; c) H. E. Katz, T. Siegrist, J. H. Schön, C. Kloc, B. Batlogg, A. J. Lovinger, J. Johnson, *ChemPhysChem* **2001**, *2*, 167.
[45] We thank P. Davidson, Laboratoire de Physique des Solides, Orsay (France) for these observations.
[46] Our own experience with chiral structures of enantiomerically pure TTF derivatives has shown that, even in the presence of pseudocentrosymmetry of the anomalous scatterers (the sulfur atoms), Flack parameters close to 0.0 were observed. We therefore consider that the 0.5 value obtained here might be a good indication of racemic twinning. See for example: a) C. Réthoré, N. Avarvari, E. Canadell, P. Auban-Senzier, M. Fourmigué, *J. Am. Chem. Soc.* **2005**, *127*, 5748; b) C. Réthoré, M. Fourmigué, N. Avarvari, *Tetrahedron* **2005**, *61*, 10935.
[47] Y. N. Kreitsberga, E. E. Liepinsh, I. B. Mazheika, O. Y. Neilands, *Vopr. Fiz. Org. Khim. Z. Org. Khim.* **1986**, *22*, 367.
[48] P. Venugopalan, K. Venkatesan, *Bull. Chem. Soc. Jpn.* **1990**, *63*, 2368.
[49] T. Devic, P. Batail, N. Avarvari, *Chem. Commun.* **2004**, 1538.
[50] G. M. J. Schmidt, *Pure Appl. Chem.* **1971**, *43*, 647.
[51] V. Ramamurthy, K. Venkatesan, *Chem. Rev.* **1987**, *87*, 433.
[52] a) A. Souizi, A. Robert, P. Batail, L. Ouahab, *J. Org. Chem.* **1987**, *52*, 1610; b) M. Giffard, P. Frère, A. Gorgues, A. Riou, J. Roncali, L. Toupet, *J. Chem. Soc. Chem. Commun.* **1993**, 944.
[53] M. Iyoda, M. Hasegawa, Y. Miyake, *Chem. Rev.* **2004**, *104*, 5085.
[54] a) J. O. Jeppesen, M. B. Nielsen, J. Becher, *Chem. Rev.* **2004**, *104*, 5115; b) M. B. Nielsen, J. Becher, *Liebigs Ann.* **1997**, 2177.
[55] D. L. Coffen, J. Q. Chambers, D. R. Williams, P. E. Garrett, N. D. Canfield, *J. Am. Chem. Soc.* **1971**, *93*, 2258.
[56] M. Iyoda, M. Hasegawa, Y. Kuwatani, H. Nishikawa, K. Fukami, N. Nagase, G. Yamamoto, *Chem. Lett.* **2001**, 1146.
[57] H. Fujiwara, E. Arai, H. Kobayashi, *J. Mater. Chem.* **1998**, *8*, 829.
[58] J. Tanabe, T. Kudo, M. Okamato, Y. Kawada, G. Ono, A. Izuoka, T. Sugawara, *Chem. Lett.* **1995**, 579.
[59] K. Takimiya, Y. Aso, F. Ogura, T. Otsubo, *Chem. Lett.* **1995**, 735.
[60] a) L. R. MacGillivray, J. L. Reid, J. A. Ripmeester, *J. Am. Chem. Soc.* **2000**, *122*, 7817; b) G. S. Papaefstathiou, A. J. Kipp, L. R. MacGillivray, *Chem. Commun.* **2001**, 2462.
[61] T. Caronna, R. Liantonio, T. A. Logothetis, P. Metrangolo, T. Pilati, G. Resnati, *J. Am. Chem. Soc.* **2004**, *126*, 4500.
[62] G. W. Coates, A. R. Dunn, L. M. Henling, D. A. Dougherty, R. H. Grubbs, *Angew. Chem.* **1996**, *108*, 290; *Angew. Chem. Int. Ed. Engl.* **1997**, *36*, 248.
[63] P. F. Schuda, C. B. Ebner, S. J. Potlock, *Synthesis* **1987**, 1055.

Received: September 1, 2005
Revised: November 16, 2005
Published online: January 27, 2006

